OPEN ACCESS
Fractals, Vol. 31, No. 10 (2023) 2340096 (17 pages)

DOI: 10.1142/S0218348X23400960

World Scientific
www.worldscientific.com

MONKEYPOX VIRAL TRANSMISSION DYNAMICS AND FRACTIONAL-ORDER MODELING WITH VACCINATION INTERVENTION

JASKIRAT PAL SINGH and SACHIN KUMAR*,†
Department of Mathematics and Statistics
Central University of Punjab
Bathinda–151401, Punjab, India
**sachin1jan@yahoo.com*

DUMITRU BALEANU†
Department of Mathematics
Cankaya University, Angara, Turkey
Institute of Space Sciences
Magurele–Bucharest, Romania
Department of Medical Research
China Medical University
Taichung, Taiwan
dumitru@cankaya.edu.tr

KOTTAKKARAN SOOPPY NISAR
Department of Mathematics, College of Arts and Sciences
Prince Sattam bin Abdulaziz University
Wadi Aldawaser, 11991, Saudi Arabia
School of Technology, Woxsen University
Hyderabad-502345, Telangana State, India

†Corresponding authors.

Received September 7, 2022
Accepted February 15, 2023
Published September 23, 2023

Abstract

A current outbreak of the monkeypox viral infection, which started in Nigeria, has spread to other areas of the globe. This affects over 28 nations, including the United Kingdom and the United States. The monkeypox virus causes monkeypox (MPX), which is comparable to smallpox and cowpox (MPXV). The monkeypox virus is a member of the Poxviridae family and belongs to the Orthopoxvirus genus. In this work, a novel fractional model for Monkeypox based on the Caputo derivative is explored. For the model, two equilibria have been established: disease-free and endemic equilibrium. Using the next-generation matrix and Castillo's technique, if $R_0 < 1$ the global asymptotic stability of disease-free equilibrium is shown. The linearization demonstrated that the endemic equilibrium point is locally asymptotically stable if $R_0 > 1$. Using the parameter values, the model's fundamental reproduction rates for both humans and non-humans are calculated. The existence and uniqueness of the solution are proved using fixed point theory. The model's numerical simulations demonstrate that the recommended actions will cause the infected people in the human and non-human populations to disappear.

Keywords: Monkeypox; Caputo Fractional Derivative; Reproduction Number; Stability Analysis; Fractional Euler's Method; Fixed Point Theory; Next-Generation Matrix; Existence and Uniqueness.

1. INTRODUCTION

In May 2022, a monkeypox epidemic was verified, beginning with a cluster of cases discovered in the United Kingdom. The first case was verified on May 6, 2022 in a person with a travel history to Nigeria (where the sickness is widespread), but it has been hypothesized that infections had been spreading throughout Europe for months before that. Cases began to be recorded from a growing number of nations and areas beginning on May 18, 2022, primarily in Europe, but also in North and South America, Asia, Africa, and Australia. As of June 8, 1285 cases have been verified from 28 countries where monkeypox is uncommon or had never been recorded.

An increasing concern to world health is monkeypox, which can spread internationally and be transmitted further. The monkeypox virus causes the infectious illness monkeypox.[1] A zoonotic virus, the monkeypox virus mostly affects rural people in Central and West Africa, especially those who live close to the tropical rainforest where exposure to infected animals is more frequent.[2] In 1959, Magnus *et al.*[3] discovered that the monkeypox virus, which is similar to the variola virus, was responsible for two epidemics of pox illnesses in long-tailed macaque that were later transported from Singapore to the Statens Serum Institut, Copenhagen, Denmark.[4] The clinical similarities between the two diseases make human monkeypox and smallpox difficult to distinguish.[2]

Even well-resourced healthcare systems with high consequence infectious diseases (HCID) networks have particular difficulties when dealing with human monkeypox. Prospective research on antivirals is urgently required to treat this condition.[5] In 1970, nine months after smallpox had been eradicated in that nation, a kid in the Democratic Republic of the Congo's (formerly Zaire) area was diagnosed with monkeypox. For more information, see Ref. 4.

By coming in touch with animal blood or being bitten, people can get monkeypox from rodents, domestic animals, and primates.[1,2] The monkeypox virus is spread when an individual comes in touch with contaminated material or person.[1] The virus can enter the body through the respiratory system, mucosal membranes, and damaged skin (eyes, nose, and mouth).[1] Animals can transmit diseases

to people via biting or scratching, coming in physical touch with diseased material such as contaminated bedding or bodily fluids, or coming in direct touch with material from wounds or biological fluids, such as compromised bedding, or direct contact with biological fluids or material from wounds. It is believed that large respiratory droplets, which can only move a limited distance and need proximity for an extended period, are the primary mechanism of human-to-human transmission.[1] Direct contact with bodily fluids is another mechanism for this group to transmit.[1]

Rarely does an illness like monkeypox leave Africa. Forty-seven confirmed or suspected cases of a zoonotic pandemic in the US were reported in 2003.[6–9] Giant rats, squirrels, and dormice from the Gambia were imported, and they later transmitted the virus to pets like prairie dogs, which is why this outbreak occurred.

The clinical disease manifests as lymphadenopathy, rash, and fever. Possible side effects of monkeypox include pneumonia, subsequent bacterial infections, encephalitis, and sight-threatening keratitis. The United States has approved the use of two orally ingestible drugs, tecovirimat and brincidofovir, to treat smallpox in the event of a bioterrorism attack, despite the fact that there are currently no licensed therapies for human monkeypox.[10–12] Although both treatments have demonstrated effectiveness in animal models against several orthopoxviruses, no human efficacy studies have been conducted on either (including monkeypox).

1.1. Description of the Model

In this paper, we propose a compartmental deterministic model of the dynamics of monkeypox transmission across two populations: humans and non-humans (certain wild rodents and/or non-human primates). The human inhabitant is additionally separated into different compartments: the susceptible $S_h(t)$, immunized $V_h(t)$, exposed $E_h(t)$, infectious $I_h(t)$, quarantined $Q_h(t)$, and recovered populations $R_h(t)$. Four categories — susceptible $S_r(t)$, exposed $E_r(t)$, infected $I_r(t)$, and recovered $R_r(t)$ — are used to categorize the non-human population. The rate of enrollment into the Homosapien inhabitant is Λ_h. A vulnerable individual has two options: either they can be inoculated from the monkeypox viral infection at rate α_h and advance to $V_h(t)$ with lifelong antibodies, or they can be infected with the disease at rate δ_h after coming into touch with a contagious human or animal as follows:

$$\delta_h = \beta_{r_2}\frac{I_r}{N_r} + \beta_h\frac{I_h}{N_h}, \tag{1}$$

where βr_2 is the actual contact rate multiplied by the likelihood that a human will get an infection from a contagious non-human per contact, and β_h is the effective contact rate multiplied by the likelihood that a human will contract the monkeypox virus from a contagious human per contact. α_1 is the fraction of exposed people who become highly infected, whereas the proportion of people who are detected and sent to isolation is α_2. Some suspected cases are verified after medical diagnosis, whereas others are not diagnosed and are reintroduced to susceptible humans at a rate ζ and τ is the rate at which cases recover from isolation. The recovery rate for humans in the infected class is ρ_h. The natural death rate in human and non-human populations is μ_h and μ_r, respectively. While d_h and d_r are the corresponding illness death rates for the human and non-human populations.

The non-humans are enlisted into the vulnerable class at a rate Λ_r a constant, and after coming in touch with a non-human who is already infected, they are exposed at a constant rate δ_r to the monkeypox virus which is determined by

$$\delta_r = \beta_{r_1}\frac{I_r}{N_r}, \tag{2}$$

where β_{r_1} denotes the actual contact rate with the likelihood of infecting a non-human per encounter with an infected non-human. Once the virus has begun to incubate, the exposed class moves forward at rate α_3 into the infected class. ρ_r represents the animal recovery rate. All of the values used for the numerical simulation are strictly non-negative and are shown in Table 1. Figure 1 depicts the conceptual structure of the model used in this paper.

1.2. Model Equations

The following model equations were generated from the model description and the schematic diagram is shown in Fig. 1.

$$S_h'(t) = \Lambda_h - (\mu_h + \delta_h + \alpha_h)S_h(t) + \zeta Q_h(t),$$
$$V_h'(t) = \alpha_h S_h(t) - \mu_h V_h(t),$$
$$E_h'(t) = \delta_h S_h(t) - (\mu_h + \alpha_1 + \alpha_2)E_h(t),$$

Table 1 Parameter Values Utilized in the Simulations.

Parameter	Value/Year	Source	Explanation
Λ_h	0.029	Bhunu and Mushayabasa[35]	Enrollment rate for humans
Λ_r	2	Bhunu and Mushayabasa[35]	Enrollment rate for non-humans
β_{r_1}	0.0027	Bhunu and Mushayabasa[35]	Contact rate for non-human to non-human interaction
β_{r_2}	0.00252	Bhunu and Mushayabasa[35]	Non-human contact rate to humans
β_h	0.000063	Bhunu and Mushayabasa[35]	Contact rate for a human to human interaction
α_1	0.2	Peter *et al.*[29]	Fraction of humans that move from exposed class to infected
α_2	2	Peter *et al.*[29]	Fraction identified as a suspected case
α_3	0.3	Usman *et al.*[34]	Fraction of exposed non-human to infected class
α_h	0.1	Usman *et al.*[34]	Fraction of susceptibles to vaccinated
ζ	0.2	Assumed	Fraction not detected after diagnosis
τ	0.52	Peter *et al.*[29]	Advancement from isolated to recovered class
μ_h	0.02	Bhunu and Mushayabasa[35]	Rate of the natural demise of human
μ_r	1.5	Bhunu and Mushayabasa[35]	Rate of natural demise for non-human
δ_r	0.4	Bhunu and Mushayabasa[35]	The death rate for non-humans due to disease
δ_h	0.1	Bhunu and Mushayabasa[35]	The death rate for humans due to disease
ρ_h	0.83	Bhunu and Mushayabasa[35]	Humans recovery rate
ρ_r	0.6	Bhunu and Mushayabasa[35]	Non-humans recovery rate

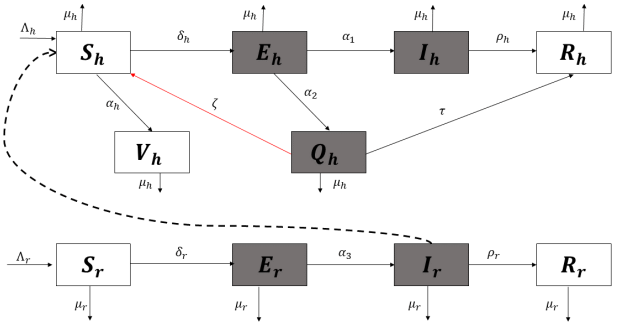

Fig. 1 Schematic model diagram.

$$
\begin{aligned}
Q_h'(t) &= \alpha_2 E_h(t) - (\zeta + \mu_h + d_h + \tau) Q_h(t),\\
I_h'(t) &= \alpha_1 E_h(t) - (\mu_h + d_h + \rho_h) I_h(t),\\
R_h'(t) &= \rho_h I_h(t) + \tau Q_h(t) - \mu_h R_h(t),\\
S_r'(t) &= \Lambda_r - (\mu_r + \delta_r) S_r(t),\\
E_r'(t) &= \delta_r S_r(t) - (\mu_r + \alpha_3) E_r(t),\\
I_r'(t) &= \alpha_3 E_r(t) - (\mu_r + d_r + \rho_r) I_r(t),\\
R_r'(t) &= \rho_r I_r(t) - \mu_r R_r(t).
\end{aligned}
\tag{3}
$$

According to the following prerequisites:

$$
\begin{aligned}
&S_h(0) \geq 0, \quad V_h(0) \geq 0, \quad E_h(0) \geq 0,\\
&Q_h(0) \geq 0, \quad I_h(0) \geq 0, \quad R_h(0) \geq 0,\\
&S_r(0) \geq 0, \quad E_r(0) \geq 0, \quad I_r(0) \geq 0, \quad R_r(0) \geq 0.
\end{aligned}
\tag{4}
$$

$$
\begin{aligned}
&S_h(t) + V_h(t) + E_h(t) + Q_h(t) + I_h(t) + R_h(t)\\
&\quad = N_h(t) \quad \text{and}\\
&S_r(t) + E_r(t) + I_r(t) + R_r(t) = N_r(t).
\end{aligned}
\tag{5}
$$

1.3. Fractional Model

To comprehend the assessment, presence, stability, and control of infectious illnesses more effectively, it is necessary to study the mathematical models of these conditions in-depth.[13–15] Because conventional mathematical models lack the high level of precision required to represent these illnesses, fractional differential equations were developed to address these issues. They are used extensively in a variety of practical domains, including cosmology, robotics, artificial intelligence, and challenges with production and optimization. For many years, mathematical models of biological phenomena have used fractional differential.[16,17] This is because integer-order models cannot adequately describe or handle various materials' retention and heritage qualities, but fractional calculus can. As a result, several angles have been used to study the aforementioned topic, including qualitative theory, numerical analysis, and more (see Refs. 16, 18 and 19). Through the use of fractional-order modeling, several researchers have extended classical calculus to the fractional order[20–22] because mathematical models are useful tools for researching infectious illnesses.

In light of the aforementioned research, we thus analyze the model (3) here under a fractional derivative in Caputo sense of order α. Additionally, in order to prevent dimensional mismatching, we change the fractional operator via the auxiliary parameter $\chi > 0$.[23,24]

$$\begin{aligned}
&\chi^{\alpha-1}D_t^\alpha[S_h(t)] \\
&\quad = \Lambda_h - (\mu_h + \delta_h + \alpha_h)S_h(t) + \zeta Q_h(t), \\
&\chi^{\alpha-1}D_t^\alpha[V_h(t)] = \alpha_h S_h(t) - \mu_h V_h(t), \\
&\chi^{\alpha-1}D_t^\alpha[E_h(t)] \\
&\quad = \delta_h S_h(t) - (\mu_h + \alpha_1 + \alpha_2)E_h(t), \\
&\chi^{\alpha-1}D_t^\alpha[Q_h(t)] \\
&\quad = \alpha_2 E_h(t) - (\zeta + \mu_h + d_h + \tau)Q_h(t), \\
&\chi^{\alpha-1}D_t^\alpha[I_h(t)] \\
&\quad = \alpha_1 E_h(t) - (\mu_h + d_h + \rho_h)I_h(t), \\
&\chi^{\alpha-1}D_t^\alpha[R_h(t)] = \rho_h I_h(t) + \tau Q_h(t) - \mu_h R_h(t), \\
&\chi^{\alpha-1}D_t^\alpha[S_r(t)] = \Lambda_r - (\mu_r + \delta_r)S_r(t), \\
&\chi^{\alpha-1}D_t^\alpha[E_r(t)] = \delta_r S_r(t) - (\mu_r + \alpha_3)E_r(t), \\
&\chi^{\alpha-1}D_t^\alpha[I_r(t)] = \alpha_3 E_r(t) - (\mu_r + d_r + \rho_r)I_r(t), \\
&\chi^{\alpha-1}D_t^\alpha[R_r(t)] = \rho_r I_r(t) - \mu_r R_r(t),
\end{aligned} \tag{6}$$

under starting conditions:

$$\begin{aligned}
&S_h(0) = S_{h0}, \quad V_h(0) = V_{h0}, \quad E_h(0) = E_{h0}, \\
&Q_h(0) = Q_{h0}, \quad I_h(0) = I_{h0}, \quad R_h(0) = R_{h0}, \\
&S_r(0) = S_{r0}, \quad E_r(0) = E_{r0}, \quad I_r(0) = I_{r0}, \\
&R_r(0) = R_{r0}.
\end{aligned} \tag{7}$$

We initially use fixed point theory to establish the existence for the solution of the proposed model. The famous modified Euler technique is then extended for numerical simulations.

The rest of the work is organized as follows:

Section 2 presents the basic definitions of fractional calculus. Section 3 is devoted to the stability analysis of the considered model. Additionally, the existence and uniqueness of the general solution of the model under consideration have been examined, as well as the best procedure for doing so utilizing the fractional Euler's technique. The suggested model's graphical representation is described in Sec. 4. Finally, Sec. 5 concludes.

2. PRELIMINARIES

Definition 1 (Ref. 25). The fractional derivative in the Caputo sense is defined as follows:

$$D^\alpha \Delta(t) = \frac{1}{\Gamma(m-\gamma)}\left[\int_0^t (t-\lambda)^{m-\gamma-1}\frac{d^m}{d\lambda^n}\Delta(\lambda)d\lambda\right],$$

where $\Delta \in \mathcal{C}^0[0,T]$, $m = \lfloor \gamma + 1 \rfloor$, and $\lfloor \gamma \rfloor$ represent an integral part of γ.

Definition 2 (Ref. 19). Riemann–Liouville fractional integral corresponding to t may be expressed as follows:

$$I^\alpha \Delta(t) = \frac{1}{\Gamma(\alpha)}\int_0^t (t-\lambda)^{\alpha-1}\Delta(\lambda)d\lambda, \quad \text{where } \alpha, \lambda \in (0,\infty),$$

where $\Delta \in \mathcal{C}^0[0,T]$ on $L_1([0,T],R)$.

3. MAIN WORK

The equilibrium points and their stability, as well as the non-negativity of the solution, are discussed in this portion. It will also be demonstrated that the suggested model's solution exists and is unique. In order to arrive at the mathematical solution to Eq. (6), we will also use the fractional Euler's approach.

3.1. Non-Negativity of the Solution

The following theorem shows the required result.

Theorem 3. *The closed set*

$$\Omega = \begin{cases} (S_h, V_h, E_h, Q_h, I_h, R_h) \\ \qquad \in \mathbb{R}_+^6 : 0 \le N_h \le \chi^{1-\alpha}\dfrac{\Lambda_h}{\mu_h} \\ (S_r, E_r, I_r, R_r) \in \mathbb{R}_+^4 : 0 \le N_r \le \chi^{1-\alpha}\dfrac{\Lambda_r}{\mu_r} \end{cases} \tag{8}$$

is positively invariant for the system (6).

Proof. Summation of first six equations of (6) gives

$$\begin{aligned}
\chi^{\alpha-1}D_t^\alpha[N_h(t)] &= \Lambda_h - \mu_h N_h - \delta_h(I_h + Q_h) \\
&\le \Lambda_h - \mu_h N_h
\end{aligned} \tag{9}$$

and summation of remaining four gives

$$\begin{aligned}
\chi^{\alpha-1}D_t^\alpha[N_r(t)] &= \Lambda_r - \mu_r N_r - \delta_r I_r \\
&\le \Lambda_r - \mu_r N_r.
\end{aligned} \tag{10}$$

When we utilized the Laplace transform on Eq. (9) as well as Eq. (10), we got the following results:

$$\begin{cases} N_h(t) \leq N_h(0)E_\alpha(-\mu_h t^\alpha) \\ \qquad\qquad + \chi^{1-\alpha}\dfrac{\Lambda_h}{\mu_h}(1 - E_\alpha(-\mu_h t^\alpha)) \\ N_r(t) \leq N_r(0)E_\alpha(-\mu_r t^\alpha) \\ \qquad\qquad + \chi^{1-\alpha}\dfrac{\Lambda_r}{\mu_r}(1 - E_\alpha(-\mu_r t^\alpha)), \end{cases} \tag{11}$$

where $N_h(0)$ and $N_r(0)$ are starting populations for the human and non-human classes, respectively. Therefore, $0 \leq N_h \leq \chi^{1-\alpha}\frac{\Lambda_h}{\mu_h}$ and $0 \leq N_r \leq \chi^{1-\alpha}\frac{\Lambda_r}{\mu_r}$ as $t \to \infty$ due to the asymptotic behavior possessed by Mittag-Leffler function E_α. This implies $\chi^{1-\alpha}\frac{\Lambda_h}{\mu_h}$ and $\chi^{1-\alpha}\frac{\Lambda_r}{\mu_r}$ are, respectively, upper limits for $N_h(t)$ and $N_r(t)$, provided $N_h(0) \leq \chi^{1-\alpha}\frac{\Lambda_h}{\mu_h}$ and $N_r(0) \leq \chi^{1-\alpha}\frac{\Lambda_r}{\mu_r}$. As a result, the model equation's (6) possible solution moves towards the positively invariant set area Ω. The system is therefore properly presented clinically and mathematically. Since the trajectory for a given initial point $x \in \Omega$ resides in Ω, it is adequate to focus our research on Ω. Thus Ω is a positive invariant set under the dynamics outlined by the model equations. □

3.2. Equilibrium Points and Stability Analysis

Equivalence points for the proposed model's equilibrium are found by setting the right side of (6) equal to 0.

$$\begin{cases} \Lambda_h - (\mu_h + \delta_h + \alpha_h)S_h(t) + \zeta Q_h(t) = 0, \\ \alpha_h S_h(t) - \mu_h V_h(t) = 0, \\ \delta_h S_h(t) - (\mu_h + \alpha_1 + \alpha_2)E_h(t) = 0, \\ \alpha_2 E_h(t) - (\zeta + \mu_h + d_h + \tau)Q_h(t) = 0, \\ \alpha_1 E_h(t) - (\mu_h + d_h + \rho_h)I_h(t) = 0, \\ \rho_h I_h(t) + \tau Q_h(t) - \mu_h R_h(t) = 0, \\ \Lambda_r - (\mu_r + \delta_r)S_r(t) = 0, \\ \delta_r S_r(t) - (\mu_r + \alpha_3)E_r(t) = 0, \\ \alpha_3 E_r(t) - (\mu_r + d_r + \rho_r)I_r(t) = 0, \\ \rho_r I_r(t) - \mu_r R_r(t) = 0. \end{cases} \tag{12}$$

The disease-free equilibrium is defined as the point at which no disease is present in the population, which is represented in the model as $E_h^0 = 0, Q_h^0 = 0, I_h^0 = 0, E_r^0 = 0, I_r^0 = 0$.

The point which is disease-free equilibrium is as follows:

$$\begin{aligned} &\epsilon^0(S_h^0, V_h^0, E_h^0, Q_h^0, I_h^0, R_h^0, S_r^0, E_r^0, I_r^0, R_r^0) \\ &= \left(\frac{\Lambda_h}{\mu_h + \alpha_h}, \frac{\Lambda_h}{\mu_h}\frac{\alpha_h}{\alpha_h + \mu_h}, 0, 0, 0, 0, \frac{\Lambda_r}{\mu_r}, 0, 0, 0\right). \end{aligned} \tag{13}$$

The endemic equilibrium state is the state where the disease cannot be totally eradicated but remains in the population. The Immunized Class, the Susceptible Class, the Latently Infected Class, the Isolated Class, the Infectious Class, and the Recovered Class must not be zero at equilibrium state for the disease to persist in the population.

Hence, the endemic equilibrium point

$$\epsilon^* = (S_h^*, V_h^*, E_h^*, Q_h^*, I_h^*, R_h^*, S_r^*, E_r^*, I_r^*, R_r^*) \tag{14}$$

can be derived by concurrently solving the equations in (12), taking into account the condition that all components of ϵ^* are non-zero.

Basic Reproduction Number

The replication number is one of the most crucial factors in evaluating an epidemic's long-term behavior. It is the total number of additional cases that a single infected person causes during the length of the infectious agent's existence. We used Diekmann *et al.*'s[26] next-generation matrix technique to obtain the expression of reproduction number R_0. and Peter *et al.*[27] and Van den Driessche *et al.*[28] were the first to present it, and they go into great depth on how to estimate R_0. The next-generation matrix technique is used in numerous papers in the literature to estimate the basic replication number expression.[29,30]

The mathematical paradigm (6) is expressed as follows: $\chi^{\alpha-1}D_t^\alpha \xi(t) = \mathbb{F}(\xi) - \mathbb{V}(\xi)$, where

$$\mathbb{F} = \begin{pmatrix} 0 \\ 0 \\ \delta_h S_h(t) \\ 0 \\ 0 \\ 0 \\ 0 \\ \delta_r S_r(t) \\ 0 \\ 0 \end{pmatrix},$$

$$\mathbb{V} = \begin{pmatrix} -\Lambda_h + (\mu_h + \delta_h + \alpha_h)S_h(t) - \zeta Q_h(t) \\ -\alpha_h S_h(t) + \mu_h V_h(t) \\ (\mu_h + \alpha_1 + \alpha_2)E_h(t) \\ -\alpha_2 E_h(t) + (\zeta + \mu_h + d_h + \tau)Q_h(t) \\ -\alpha_1 E_h(t) + (\mu_h + d_h + \rho_h)I_h(t) \\ -\rho_h I_h(t) - \tau Q_h(t) + \mu_h R_h(t) \\ -\Lambda_r + (\mu_r + \delta_r)S_r(t) \\ (\mu_r + \alpha_3)E_r(t) \\ -\alpha_3 E_r(t) + (\mu_r + d_r + \rho_r)I_r(t) \\ -\rho_r I_r(t) + \mu_r R_r(t) \end{pmatrix}. \tag{15}$$

It is not thought of as a fresh infection when a person progresses from E_h to Q_h or I_h; rather, it is the evolution of ill people across several compartments. In light of this, the transmissions matrix F and the transitions matrix V are

$$F = \begin{pmatrix} 0 & 0 & \beta_h & 0 & \beta_{r_2} \\ 0 & 0 & 0 & 0 & 0 \\ 0 & 0 & 0 & 0 & 0 \\ 0 & 0 & 0 & \beta_{r_1} & 0 \\ 0 & 0 & 0 & 0 & 0 \end{pmatrix},$$

$$V = \begin{pmatrix} \mu_h + \alpha_1 + \alpha_2 & 0 & 0 & 0 & 0 \\ -\alpha_2 & \rho_h + d_h + \mu_h + \tau & 0 & 0 & 0 \\ -\alpha_1 & 0 & \mu_h + d_h + \rho_h & 0 & 0 \\ 0 & 0 & 0 & \mu_r + \alpha_3 & 0 \\ 0 & 0 & 0 & -\alpha_3 & \mu_r + d_r + \rho_r \end{pmatrix}.$$

For simplicity, let $\Psi_1 = \mu_h + \alpha_1 + \alpha_2, \Psi_2 = \rho_h + d_h + \mu_h + \tau, \Psi_3 = \mu_h + d_h + \rho_h, \Psi_4 = \mu_r + \alpha_3, \Psi_5 = \mu_r + d_r + \rho_r$.

So we have,

$$V^{-1} = \begin{pmatrix} \frac{1}{\Psi_1} & 0 & 0 & 0 & 0 \\ \frac{\alpha_2}{\Psi_1\Psi_2} & \frac{1}{\Psi_2} & 0 & 0 & 0 \\ \frac{\alpha_1}{\Psi_1\Psi_3} & 0 & \frac{1}{\Psi_3} & 0 & 0 \\ 0 & 0 & 0 & \frac{1}{\Psi_4} & 0 \\ 0 & 0 & 0 & \frac{\alpha_3}{\Psi_4\Psi_5} & \frac{1}{\Psi_5} \end{pmatrix}. \tag{16}$$

So,

$$FV^{-1} = \begin{pmatrix} \frac{\beta_h\alpha_1}{\Psi_1\Psi_3} & 0 & \frac{\beta_h}{\Psi_3} & \frac{\beta_{r_2}\alpha_3}{\Psi_4\Psi_5} & \frac{\beta_{r_2}}{\Psi_5} \\ 0 & 0 & 0 & 0 & 0 \\ 0 & 0 & 0 & 0 & 0 \\ 0 & 0 & 0 & \frac{\beta_{r_1}}{\Psi_4} & 0 \\ 0 & 0 & 0 & 0 & 0 \end{pmatrix}. \tag{17}$$

Hence, R_0 of the model is given by

$$R_0 = \{R_{0,h}, R_{0,r}\},$$

where R_h and R_r are the numbers of monkeypox-induced reproduction in humans and non-humans, respectively, and are given by

$$R_{0,h} = \frac{\beta_h\alpha_1}{(\mu_h + \alpha_1 + \alpha_2)(\mu_h + d_h + \rho_h)}, \tag{18}$$

$$R_{0,r} = \frac{\beta_{r_1}}{(\mu_r + \alpha_3)}. \tag{19}$$

Stability of Disease-Free Equilibrium

Using the modified version of technique proposed by Castillo-Chavez *et al.*[31] to determine the requirements for global stability for ϵ^0, the model system (6) may be expressed as follows:

$$\begin{aligned} &\chi^{\alpha-1}D_t^\alpha Y = K(Y,U), \\ &\chi^{\alpha-1}D_t^\alpha U = P(Y,U), \quad P(Y,0) = 0, \end{aligned} \tag{20}$$

where $U \in \mathbb{R}^n$ represents the total number of infected people, including exposed, contagious, etc., and $Y \in \mathbb{R}^m$ represents the total number of uninfected people. This system's disease-free equilibrium is indicated by $\epsilon^0 = (y^0; 0)$. To ensure local asymptotic stability, the requirements (S1) and (S2) must be satisfied.

(S1) For $\chi^{\alpha-1}D_t^\alpha Y = K(Y,0), Y^*$ is globally asymptotically stable,

(S2) $P(Y,U) = BU - \hat{P}(Y,U); \hat{P}(Y;U) \geq 0$ for $(Y,U) \in \Omega$, where $B = D_U P(Y^0, 0)$ is a matrix whose elements other than elements on the diagonal of B are positive or zero and is the domain in which model makes medical sense.

Lemma 4. *The point $\epsilon^0 = (y^0, 0)$ is an asymptotic stable equilibrium globally of (20) given that $R_0 < 1$ and that (S1) and (S2) hold.*

We may use this lemma for fractional derivatives by altering the derivatives. The global stability of the DFE ϵ^0 for the suggested model is shown by the theorem below.

Theorem 5. *The ϵ^0 DFE is asymptotically stable globally provided $R_0 \leq 1$.*

Proof. First, we will prove S1 as follows:

$$K(Y,0) = \begin{bmatrix} \Lambda_h - (\mu_h + \alpha_h)S_h \\ \alpha_h S_h - \mu_h V_h \\ -\mu_h R_h \\ \Lambda_r - \mu_r S_r \\ -\mu_r R_r \end{bmatrix}.$$

The characteristic polynomial is

$$(\mu_h + \lambda)^2(\mu_h + \alpha_h + \lambda)(\mu_r + \lambda)^2 \tag{21}$$

$\Rightarrow \lambda_1 = \lambda_2 = -\mu_h, \lambda_3 = -(\mu_h + \alpha_h), \lambda_4 = \lambda_5 = -\mu_r$. Hence, $Y = Y^0$ is globally stable.

Now, we have

$$P(Y,U) = BU - \hat{P}(Y,U)$$

$$= \begin{bmatrix} -(\mu_h + \alpha_1 + \alpha_2) & 0 & \frac{\beta_h S_h^0}{N_h} & 0 & \frac{\beta_{r_2} S_r^0}{N_r} \\ \alpha_2 & -(\zeta + \mu_h + d_h + \tau) & 0 & 0 & 0 \\ \alpha_1 & 0 & -(\mu_h + d_h + \rho_h) & 0 & 0 \\ 0 & 0 & 0 & -(\mu_r + \alpha_3) & \frac{\beta_{r_1} S_r^0}{N_r} \\ 0 & 0 & 0 & \alpha_3 & -(\mu_r + d_r + \rho_r) \end{bmatrix}$$

$$\times \begin{bmatrix} E_h \\ Q_h \\ I_h \\ E_r \\ I_R \end{bmatrix} + \begin{bmatrix} \frac{\beta_{r_2}(S_r - S_r^0)}{N_r} I_r + \frac{\beta_h (S_h - S_h^0)}{N_h} I_h \\ 0 \\ 0 \\ \frac{\beta_{r_1}(S_r - S_r^0)}{N_r} I_r \\ 0 \end{bmatrix}. \tag{22}$$

Here, one can easily observe that B satisfies condition S2. □

Stability of Endemic Equilibrium

The Routh–Hurwitz criteria[32] will be used to prove the endemic equilibria's local stability. In this case, it will be determined under what conditions the epidemic equilibrium is asymptotically stable. The following is the Jacobian matrix for the endemic equilibrium ϵ^*:

$$J = \begin{bmatrix} a_{(1,1)} & 0 & 0 & a_{(1,4)} & a_{(1,5)} & 0 & 0 & 0 & a_{(1,9)} & 0 \\ a_{(2,1)} & a_{(2,2)} & 0 & 0 & 0 & 0 & 0 & 0 & 0 & 0 \\ a_{(3,1)} & 0 & a_{(3,3)} & 0 & a_{(3,5)} & 0 & 0 & 0 & a_{(3,9)} & 0 \\ 0 & 0 & a_{(4,3)} & a_{(4,4)} & 0 & 0 & 0 & 0 & 0 & 0 \\ 0 & 0 & a_{(5,3)} & 0 & a_{(5,5)} & 0 & 0 & 0 & 0 & 0 \\ 0 & 0 & 0 & a_{(6,4)} & a_{(6,5)} & a_{(6,6)} & 0 & 0 & 0 & 0 \\ 0 & 0 & 0 & 0 & 0 & 0 & a_{(7,7)} & 0 & a_{(7,9)} & 0 \\ 0 & 0 & 0 & 0 & 0 & 0 & a_{(8,7)} & a_{(8,8)} & a_{(8,9)} & 0 \\ 0 & 0 & 0 & 0 & 0 & 0 & 0 & a_{(9,8)} & a_{(9,9)} & 0 \\ 0 & 0 & 0 & 0 & 0 & 0 & 0 & 0 & a_{(10,9)} & a_{(10,10)} \end{bmatrix}. \tag{23}$$

Here,

$$a_{(1,1)} = -(\mu_h + \delta_h + \alpha_h), \quad a_{(1,4)} = \zeta,$$
$$a_{(1,5)} = \frac{-\beta_h S_h}{N_h},$$
$$a_{(1,9)} = \frac{-\beta_{r_2} S_h}{N_r} a_{(2,1)} = \alpha_h, \quad a_{(2,2)} = -\mu_h,$$
$$a_{(3,1)} = \delta_h,$$
$$a_{(3,3)} = -(\mu_h + \alpha_1 + \alpha_2), \quad a_{(3,5)} = \frac{\beta_h S_h}{N_h},$$
$$a_{(3,9)} = \frac{\beta_r S_h}{N_r},$$
$$a_{(4,3)} = \alpha_2, \quad a_{(4,4)} = -(\zeta + \mu_h + d_h + \tau),$$
$$a_{(5,3)} = \alpha_1,$$
$$a_{(5,5)} = (\mu_h + d_h + \rho_h), \quad a_{(6,4)} = \tau,$$
$$a_{(6,5)} = \rho_h,$$
$$a_{(6,6)} = -\mu_h, \quad a_{(7,7)} = -(\mu_r + \delta_r),$$
$$a_{(7,9)} = \frac{-\beta_{r_1} S_r}{N_r},$$
$$a_{(8,7)} = \delta_r, \quad a_{(8,8)} = -(\mu_r + \alpha_3),$$
$$a_{(8,9)} = \frac{\beta_{r_1} S_r}{N_r},$$
$$a_{(9,8)} = \alpha_3, a_{(9,9)} = -(\mu_r + d_r + \rho_r),$$
$$a_{(10,9)} = \rho_r,$$
$$a_{(10,10)} = -\mu_r.$$

The characteristic equation of J is given as follows:

$$\begin{aligned}
&(\lambda - a_{(10,10)})(\lambda - a_{(2,2)})(\lambda - a_{(6,6)}) \\
&\quad \times (\lambda^4 + (-a_{(5,5)} - a_{(1,1)} - a_{(4,4)} - a_{(3,3)})\lambda^3 \\
&\quad + ((a_{(5,5)} + a_{(3,3)} + a_{(1,1)})a_{(4,4)} \\
&\quad + a_{(5,5)} + a_{(3,3)})a_{(1,1)} - a_{(3,5)}a_{(5,3)} \\
&\quad + a_{(3,3)}a_{(5,5)})\lambda^2 + (((-a_{(5,5)} - a_{(3,3)})a_{(1,1)} \\
&\quad + a_{(3,5)}a_{(5,3)} - a_{(3,3)}a_{(5,5)})a_{(4,4)} + (a_{(3,5)}a_{(5,3)} \\
&\quad - a_{(3,3)}a_{(5,5)})a_{(1,1)} - a_{(3,1)}(a_{(5,3)}a_{(1,5)} \\
&\quad + a_{(1,4)}a_{(4,3)}))\lambda + ((-a_{(3,5)}a_{(5,3)} + a_{(3,3)}a_{(5,5)}) \\
&\quad \times a_{(1,1)} + a_{(5,3)}a_{(3,1)}a_{(1,5)})a_{(4,4)} + a_{(3,1)}a_{(1,4)} \\
&\quad \times a_{(4,3)}a_{(5,5)})(\lambda^3 + (-a_{(7,7)} - a_{(9,9)} - a_{(8,8)})\lambda^2 \\
&\quad + ((a_{(8,8)} + a_{(9,9)})a_{(7,7)} + a_{(9,9)}a_{(8,8)} \\
&\quad - a_{(9,8)}a_{(8,9)})\lambda + (-a_{(9,9)}a_{(8,8)} + a_{(9,8)}a_{(8,9)}) \\
&\quad \times a_{(7,7)} - a_{(7,9)}a_{(9,8)}a_{(8,7)}). \qquad (24)
\end{aligned}$$

Changing Eq. (24) to the standard form, we get

$$x^{10} + B_1 x^9 + B_2 x^8 + B_3 x^7 + B_4 x^6 + B_5 x^5 + B_6 x^4 + B_7 x^3 + B_8 x^2 + B_9 x + B_{10}. \qquad (25)$$

Theorem 6 (Ref. 29). *The endemic equilibrium point is locally asymptotically stable provided* $R_0 > 1$ *and if the real component of every root of the characteristic equation is negative.*

3.3. Existence and Uniqueness of the Solution

To verify that the solution of the fractional model (6) exists and is unique, we shall apply the fixed point theory. For this reason, the fractional system (6) is written as follows:

$$\begin{cases} \chi^{\alpha-1} D_t^{\alpha} l(t) = \mathfrak{X}(t, l(t)), \\ l(0) = l_0, \quad 0 \le t \le \mathfrak{T} \le \infty. \end{cases} \qquad (26)$$

The vector $l(t) = (S_h, V_h, E_h, Q_h, I_h, R_h, S_r, E_r, I_r, R_r)$ in the system (26) contains state variables and $\mathfrak{G}$ represents a continuous vector function defined as follows:

$$\mathfrak{X} = \begin{pmatrix} \mathfrak{X}_1 \\ \mathfrak{X}_2 \\ \mathfrak{X}_3 \\ \mathfrak{X}_4 \\ \mathfrak{X}_5 \\ \mathfrak{X}_6 \\ \mathfrak{X}_7 \\ \mathfrak{X}_8 \\ \mathfrak{X}_9 \\ \mathfrak{X}_{10} \end{pmatrix} = \begin{pmatrix} \Lambda_h - (\mu_h + \delta_h + \alpha_h)S_h(t) + \zeta Q_h(t) \\ \alpha_h S_h(t) - \mu_h V_h(t) \\ \delta_h S_h(t) - (\mu_h + \alpha_1 + \alpha_2)E_h(t) \\ \alpha_2 E_h(t) - (\zeta + \mu_h + d_h + \tau)Q_h(t) \\ \alpha_1 E_h(t) - (\mu_h + d_h + \rho_h)I_h(t) \\ \rho_h I_h(t) + \tau Q_h(t) - \mu_h R_h(t) \\ \Lambda_r - (\mu_r + \delta_r)S_r(t) \\ \delta_r S_r(t) - (\mu_r + \alpha_3)E_r(t) \\ \alpha_3 E_r(t) - (\mu_r + d_r + \rho_r)I_r(t) \\ \rho_r I_r(t) - \mu_r R_r(t) \end{pmatrix}.$$

The beginning state for state variables is $l_0(t) = (S_h(0),\ V_h(0),\ E_h(0),\ Q_h(0),\ I_h(0),\ R_h(0),\ S_r(0),\ E_r(0), I_r(0),\ R_r(0))$. The Lipschitz requirement is also met by $\mathfrak{X}$ as follows:

$$\|\mathfrak{X}(t, l_1(t)) - \mathfrak{X}(t, l_2(t))\| \leq \mathcal{N}\|l_1(t) - l_2(t)\|. \quad (27)$$

The following theorem will be used to verify the existence and uniqueness of the solution for the fractional model system (6):

Theorem 7. *If the condition given below holds, the proposed model* (6) *has a unique solution*:

$$\frac{\chi^{\alpha}}{\Gamma(\alpha)}\mathcal{N}\mathfrak{T}^{\alpha}_{\max} < 1. \quad (28)$$

Proof. To get the Volterra integral equation, we use fractional integral (2) on both sides of the model (26):

$$l(t) = l_0 + \frac{\chi^{1-\alpha}}{\Gamma(\alpha)}\int_0^t (t-\lambda)^{\alpha-1}\mathfrak{X}(\lambda, l(\lambda))d\lambda. \quad (29)$$

Let $W = (0, \mathfrak{T})$ and the function $\Sigma : \mathcal{C}(W, \mathbb{R}^{10}) \to \mathcal{C}(W, \mathbb{R}^{10})$ is stated as follows:

$$\Sigma[l(t)] = l_0 + \frac{\chi^{1-\alpha}}{\Gamma(\alpha)}\int_0^t (t-\lambda)^{\alpha-1}\mathfrak{X}(\lambda, l(\lambda))d\lambda. \quad (30)$$

Equation (29) becomes

$$l(t) = \Sigma[l(t)]. \quad (31)$$

The norm $\|.\|_W$ is

$$\|l(t)\|_W = \sup_{t\in W}\|l(t)\|, \quad l(t) \in \mathcal{C}. \quad (32)$$

A Banach space is formed by $\mathcal{C}(W, \mathbb{R}^{10})$ with the norm $\|.\|_W$. Also, the following inequality holds:

$$\left\|\int_0^t \mathfrak{H}(t,\lambda)l(\lambda)d\lambda\right\| \leq \mathfrak{T}\|\mathfrak{H}(t,\lambda)\|_W\|l(t)\|_W, \quad (33)$$

with $l(t) \in \mathcal{C}(W, \mathbb{R}^{10}), \mathfrak{H}(t,\lambda) \in \mathcal{C}(W^2, \mathbb{R})$ such that

$$\|\mathfrak{H}(t,\lambda)\|_W = \sup_{t,\lambda\in W}|\mathfrak{H}(t,\lambda)|. \quad (34)$$

Using Eq. (31), we get

$$\|\Sigma[l_1(t)] - \Sigma[l_2(t)]\|_W \leq \left\|\frac{\chi^{1-\alpha}}{\Gamma(\alpha)}\int_0^t (t-\lambda)^{\alpha-1}(\mathfrak{X}(\lambda, l_1(\lambda)) - \mathfrak{X}(\lambda, l_2(\lambda)))d\lambda\right\|_W. \quad (35)$$

Equation (35) may be simplified as follows with the use of Eqs. (27), (33), and also triangular inequality:

$$\|\Sigma[l_1(t)] - \Sigma[l_2(t)]\|_W \leq \frac{\chi^{1-\alpha}}{\Gamma(\alpha)}\mathcal{N}\mathfrak{T}^{\alpha}_{\max}\|l_1(t) - l_2(t)\|_W. \quad (36)$$

Hence, we get the result

$$\|\Sigma[l_1(t)] - \Sigma[l_2(t)]\|_W \leq \mathbb{D}\|l_1(t) - l_2(t)\|_W, \quad (37)$$

where

$$\mathbb{D} = \frac{1}{\Gamma(\alpha)}\mathcal{N}\mathfrak{T}^{\alpha}_{\max}.$$

The operator Σ follows the condition in Eq. (28), therefore it is a contraction mapping. Hence, the solution is unique for the system (26). □

4. NUMERICAL SIMULATION AND GRAPHS

4.1. Numerical Scheme

Here, we develop the general technique for our model under consideration using the fractional-order Euler method. Rewriting (6) as follows:

$$\begin{cases} \chi^{\alpha-1}D^{\alpha}_t[S_h(t)] = \Theta_1(t, S_h(t)), \\ \chi^{\alpha-1}D^{\alpha}_t[V_h(t)] = \Theta_2(t, V_h(t)), \\ \chi^{\alpha-1}D^{\alpha}_t[E_h(t)] = \Theta_3(t, E_h(t)), \\ \chi^{\alpha-1}D^{\alpha}_t[Q_h(t)] = \Theta_4(t, Q_h(t)), \\ \chi^{\alpha-1}D^{\alpha}_t[I_h(t)] = \Theta_5(t, I_h(t)), \\ \chi^{\alpha-1}D^{\alpha}_t[R_h(t)] = \Theta_6(t, R_h(t)), \\ \chi^{\alpha-1}D^{\alpha}_t[S_r(t)] = \Theta_7(t, S_r(t)), \\ \chi^{\alpha-1}D^{\alpha}_t[E_r(t)] = \Theta_8(t, E_r(t)), \\ \chi^{\alpha-1}D^{\alpha}_t[I_r(t)] = \Theta_9(t, I_r(t)), \\ \chi^{\alpha-1}D^{\alpha}_t[R_r(t)] = \Theta_{10}(t, R_r(t), \end{cases} \quad (38)$$

where

$$\begin{cases} \Theta_1(t, S_h(t)) \\ \qquad = \Lambda_h - (\mu_h + \delta_h + \alpha_h)S_h(t) + \zeta Q_h(t), \\ \Theta_2(t, V_h(t)) = \alpha_h S_h(t) - \mu_h V_h(t), \\ \Theta_3(t, E_h(t)) \\ \qquad = \delta_h S_h(t) - (\mu_h + \alpha_1 + \alpha_2)E_h(t), \\ \Theta_4(t, Q_h(t)) \\ \qquad = \alpha_2 E_h(t) - (\zeta + \mu_h + d_h + \tau)Q_h(t), \end{cases}$$

$$\begin{cases}\Theta_5(t, I_h(t)) = \alpha_1 E_h(t) - (\mu_h + d_h + \rho_h) I_h(t),\\ \Theta_6(t, R_h(t)) = \rho_h I_h(t) + \tau Q_h(t) - \mu_h R_h(t),\\ \Theta_7(t, S_r(t)) = \Lambda_r - (\mu_r + \delta_r) S_r(t),\\ \Theta_8(t, E_r(t)) = \delta_r S_r(t) - (\mu_r + \alpha_3) E_r(t),\\ \Theta_9(t, I_r(t)) = \alpha_3 E_r(t) - (\mu_r + d_r + \rho_r) I_r(t),\\ \Theta_{10}(t, R_r(t) = \rho_r I_r(t) - \mu_r R_r(t).\end{cases} \tag{39}$$

To create an iterative method, we proceed as follows with Eq. (1) of the mathematical model (6):

$$\begin{cases}\chi^{\alpha-1} D_t^{\alpha}[S_h(t)] = \Theta_1(t, S_h(t)),\\ S_h(0) = S_{h0}, \quad t > 0.\end{cases} \tag{40}$$

Let $[0, a]$ represent the set of points at which we are trying to solve Eq. (40). Actually, we are unable to evaluate the function $S_h(t)$, which is required to solve Eq. (40). Instead, a collection of points (t_m, t_{m+1}) is formed and utilized as the basis for an iterative process. To do this, let us use the nodes $t_m = mh$ for $m = 0, 1, 2, ..., k$ to split the interval $[0, a]$ into k parts $[t_m, t_{m+1}]$ with identical length $h = ak$. $S_h(t)$, $D_t^{\alpha}[S_h(t)]$, and $D_t^{2\alpha}[S_h(t)]$ are assumed to be continuous on $[0, a]$. Extend the generalized Taylor formula's $S_h(t)$ to the value of $t = t_0 = 0$. There is a value C_1 for every value t ensuring that

$$S_h(t) = S_h(t_0) + D_t^{\alpha}[S_h(t)]t_0 \frac{t^{\alpha}}{\Gamma(\alpha+1)} + D_t^{2\alpha}[S_h(t)]C_1 \frac{t^{2\alpha}}{\Gamma(2\alpha+1)}, \tag{41}$$

when $D_t^{\alpha}[S_h(t)]t_0 = \chi^{1-\alpha}\Theta_1(t_0, S_h(t_0))$ and $t = h = t_1$ are substituted in (41), the resulting expression is

$$S_h(t_1) = S_h(t_0) + \chi^{1-\alpha}\Theta_1(t_0, S_h(t_0))\frac{h^{\alpha}}{\Gamma(\alpha+1)} + D_t^{2\alpha}[S_h(t)]C_1 \frac{h^{2\alpha}}{\Gamma(2\alpha+1)}.$$

We can disregard the second-order term $(h^{2\alpha})$ if h is negligible and get

$$S_h(t_1) = S_h(t_0) + \chi^{1-\alpha}\Theta_1(t_0, S_h(t_0))\frac{h^{\alpha}}{\Gamma(\alpha+1)}. \tag{42}$$

A series of points that approximates the answer is generated by repeating the process in the same way. The following is a general formula for fractional Euler's method about $t_{m+1} = t_m + h$,

$$S_h(t_{m+1}) = S_h(t_m) + \chi^{1-\alpha}\Theta_1(t_m, S_h(t_m)) \times \frac{h^{\alpha}}{\Gamma(\alpha+1)}. \tag{43}$$

We will now derive the fundamental algorithm for solving Eq. (40) numerically. Taking the fractional integral and applying it to both sides of (40), we get

$$S_h(t) = S_h(0) + I^{\alpha}[\chi^{1-\alpha}\Theta_1(t, S_h(t))]. \tag{44}$$

To obtain the solution point $(t_1, S_h(t_1))$, we substitute $t = t_1$ into (44) and we get

$$S_h(t_1) = S_h(0) + I^{\alpha}([\Theta_1(t, S_h(t))])(t_1). \tag{45}$$

Now, if $(I^{\alpha}([\Theta_1(t, S_h(t))])(t_1)$ is approximated using the modified trapezoidal method with step size $h = t_1 t_0$, Eq. (44) becomes

$$S_h(t_1) = S_h(0) + \frac{\alpha h^{\alpha}[\chi^{1-\alpha}\Theta_1(t_0, S_h(t_0))]}{\Gamma(\alpha+2)} + \frac{\alpha h^{\alpha}[\chi^{1-\alpha}\Theta_1(t_1, S_h(t_1))]}{\Gamma(\alpha+2)}. \tag{46}$$

It is important to note that the right side of Equation (46) contains $S_h(t_1)$. As a result, we use an estimate for $S_h(t_1)$. Substituting (42) into (46) yields

$$S_h(t_1) = S_h(0) + \frac{\alpha h^{\alpha}[\chi^{1-\alpha}\Theta_1(t_0, S_h(t_0))]}{\Gamma(\alpha+2)} + \frac{h^{\alpha}[\chi^{1-\alpha}\Theta_1(t_1, S_h(t_0))] + \frac{h_{\alpha}}{\Gamma(\alpha+2)}\chi^{1-\alpha}\Theta_1(t_0, S_h(t_0))}{\Gamma(\alpha+2)}. \tag{47}$$

Until a collection of points that resembles the $S_h(t)$ is obtained, the procedure is repeated. Our algorithm's general formula is as follows:

$$\begin{cases} S_h(t_m) = S_h(0) + \chi^{1-\alpha}\frac{h^{\alpha}}{\Gamma(\alpha+2)}\big((m-1)^{\alpha+1} - (m-\alpha-1)m^{\alpha}\big)\Theta_1(t_0, S_h(t_0))\\ \quad + \chi^{1-\alpha}\frac{h^{\alpha}}{\Gamma(\alpha+2)}\sum_{i=1}^{m-1}((m-i+1)^{\alpha+1}\\ \quad - 2(m-1)^{\alpha+1} + (m-i-1)^{\alpha+1})\Theta_1\\ \quad \times (t_i, S_h(t_i)) + \chi^{1-\alpha}\frac{h^{\alpha}}{\Gamma(\alpha+2)}\Theta_1\\ \quad \times \left(t_m, S_h(t_{m-1}) + \frac{h_{\alpha}}{\Gamma(\alpha+2)}\Theta_1\right.\\ \quad \left.\times (t_{m-1}, S_h(t_{m-1}))\right). \end{cases} \tag{48}$$

Using the same method as described above, we generate the numerical estimate for the model (6)'s remaining compartments.

$$\begin{cases} V_h(t_m) = V_h(0) + \chi^{1-\alpha}\dfrac{h^\alpha}{\Gamma(\alpha+2)}\big((m-1)^{\alpha+1} \\ \quad -(m-\alpha-1)m^\alpha\big)\Theta_2(t_0, V_h(t_0)) \\ \quad +\chi^{1-\alpha}\dfrac{h^\alpha}{\Gamma(\alpha+2)}\displaystyle\sum_{i=1}^{m-1}\big((m-i+1)^{\alpha+1} \\ \quad -2(m-1)^{\alpha+1}+(m-i-1)^{\alpha+1}\big)\Theta_2 \\ \quad \times(t_i, V_h(t_i)) + \chi^{1-\alpha}\dfrac{h^\alpha}{\Gamma(\alpha+2)}\Theta_2 \\ \quad \times\left(t_m, V_h(t_{m-1}) + \dfrac{h^\alpha}{\Gamma(\alpha+2)}\Theta_2 \right. \\ \quad \left. \times(t_{m-1}, V_h(t_{m-1}))\right), \end{cases} \tag{49}$$

$$\begin{cases} E_h(t_m) = E_h(0) + \chi^{1-\alpha}\dfrac{h^\alpha}{\Gamma(\alpha+2)}\big((m-1)^{\alpha+1} \\ \quad -(m-\alpha-1)m^\alpha\big)\Theta_3(t_0, E_h(t_0)) \\ \quad +\chi^{1-\alpha}\dfrac{h^\alpha}{\Gamma(\alpha+2)}\displaystyle\sum_{i=1}^{m-1}\big((m-i+1)^{\alpha+1} \\ \quad -2(m-1)^{\alpha+1}+(m-i-1)^{\alpha+1}\big)\Theta_3 \\ \quad \times(t_i, E_h(t_i)) + \chi^{1-\alpha}\dfrac{h^\alpha}{\Gamma(\alpha+2)}\Theta_3 \\ \quad \times\left(t_m, E_h(t_{m-1}) + \dfrac{h^\alpha}{\Gamma(\alpha+2)}\Theta_3 \right. \\ \quad \left. \times(t_{m-1}, E_h(t_{m-1}))\right), \end{cases} \tag{50}$$

$$\begin{cases} Q_h(t_m) = Q_h(0) + \chi^{1-\alpha}\dfrac{h^\alpha}{\Gamma(\alpha+2)}\big((m-1)^{\alpha+1} \\ \quad -(m-\alpha-1)m^\alpha\big)\Theta_4(t_0, Q_h(t_0)) \\ \quad +\chi^{1-\alpha}\dfrac{h^\alpha}{\Gamma(\alpha+2)}\displaystyle\sum_{i=1}^{m-1}\big((m-i+1)^{\alpha+1} \\ \quad -2(m-1)^{\alpha+1}+(m-i-1)^{\alpha+1}\big)\Theta_4 \\ \quad \times(t_i, Q_h(t_i)) + \chi^{1-\alpha}\dfrac{h^\alpha}{\Gamma(\alpha+2)}\Theta_4 \\ \quad \times\left(t_m, Q_h(t_{m-1}) + \dfrac{h^\alpha}{\Gamma(\alpha+2)}\Theta_4 \right. \\ \quad \left. \times(t_{m-1}, Q_h(t_{m-1}))\right), \end{cases} \tag{51}$$

$$\begin{cases} I_h(t_m) = I_h(0) + \chi^{1-\alpha}\dfrac{h^\alpha}{\Gamma(\alpha+2)}\big((m-1)^{\alpha+1} \\ \quad -(m-\alpha-1)m^\alpha\big)\Theta_5(t_0, I_h(t_0)) \\ \quad +\chi^{1-\alpha}\dfrac{h^\alpha}{\Gamma(\alpha+2)}\displaystyle\sum_{i=1}^{m-1}\big((m-i+1)^{\alpha+1} \\ \quad -2(m-1)^{\alpha+1}+(m-i-1)^{\alpha+1}\big)\Theta_5 \\ \quad \times(t_i, I_h(t_i)) + \chi^{1-\alpha}\dfrac{h^\alpha}{\Gamma(\alpha+2)}\Theta_5 \\ \quad \times\left(t_m, I_h(t_{m-1}) + \dfrac{h^\alpha}{\Gamma(\alpha+2)}\Theta_5 \right. \\ \quad \left. \times(t_{m-1}, I_h(t_{m-1}))\right), \end{cases} \tag{52}$$

$$\begin{cases} R_h(t_m) = R_h(0) + \chi^{1-\alpha}\dfrac{h^\alpha}{\Gamma(\alpha+2)}\big((m-1)^{\alpha+1} \\ \quad -(m-\alpha-1)m^\alpha\big)\Theta_6(t_0, R_h(t_0)) \\ \quad +\chi^{1-\alpha}\dfrac{h^\alpha}{\Gamma(\alpha+2)}\displaystyle\sum_{i=1}^{m-1}\big((m-i+1)^{\alpha+1} \\ \quad -2(m-1)^{\alpha+1}+(m-i-1)^{\alpha+1}\big)\Theta_6 \\ \quad \times(t_i, R_h(t_i)) + \chi^{1-\alpha}\dfrac{h^\alpha}{\Gamma(\alpha+2)}\Theta_6 \\ \quad \times\left(t_m, R_h(t_{m-1}) + \dfrac{h^\alpha}{\Gamma(\alpha+2)}\Theta_6 \right. \\ \quad \left. \times(t_{m-1}, R_h(t_{m-1}))\right), \end{cases} \tag{53}$$

$$\begin{cases} S_r(t_m) = S_r(0) + \chi^{1-\alpha}\dfrac{h^\alpha}{\Gamma(\alpha+2)}\big((m-1)^{\alpha+1} \\ \quad -(m-\alpha-1)m^\alpha\big)\Theta_7(t_0, S_r(t_0)) \\ \quad +\chi^{1-\alpha}\dfrac{h^\alpha}{\Gamma(\alpha+2)}\displaystyle\sum_{i=1}^{m-1}\big((m-i+1)^{\alpha+1} \\ \quad -2(m-1)^{\alpha+1}+(m-i-1)^{\alpha+1}\big) \\ \quad \times\Theta_7(t_i, S_r(t_i)) + \chi^{1-\alpha}\dfrac{h^\alpha}{\Gamma(\alpha+2)}\Theta_7 \\ \quad \times\left(t_m, S_r(t_{m-1}) + \dfrac{h^\alpha}{\Gamma(\alpha+2)} \right. \\ \quad \left. \times\Theta_7(t_{m-1}, S_r(t_{m-1}))\right), \end{cases} \tag{54}$$

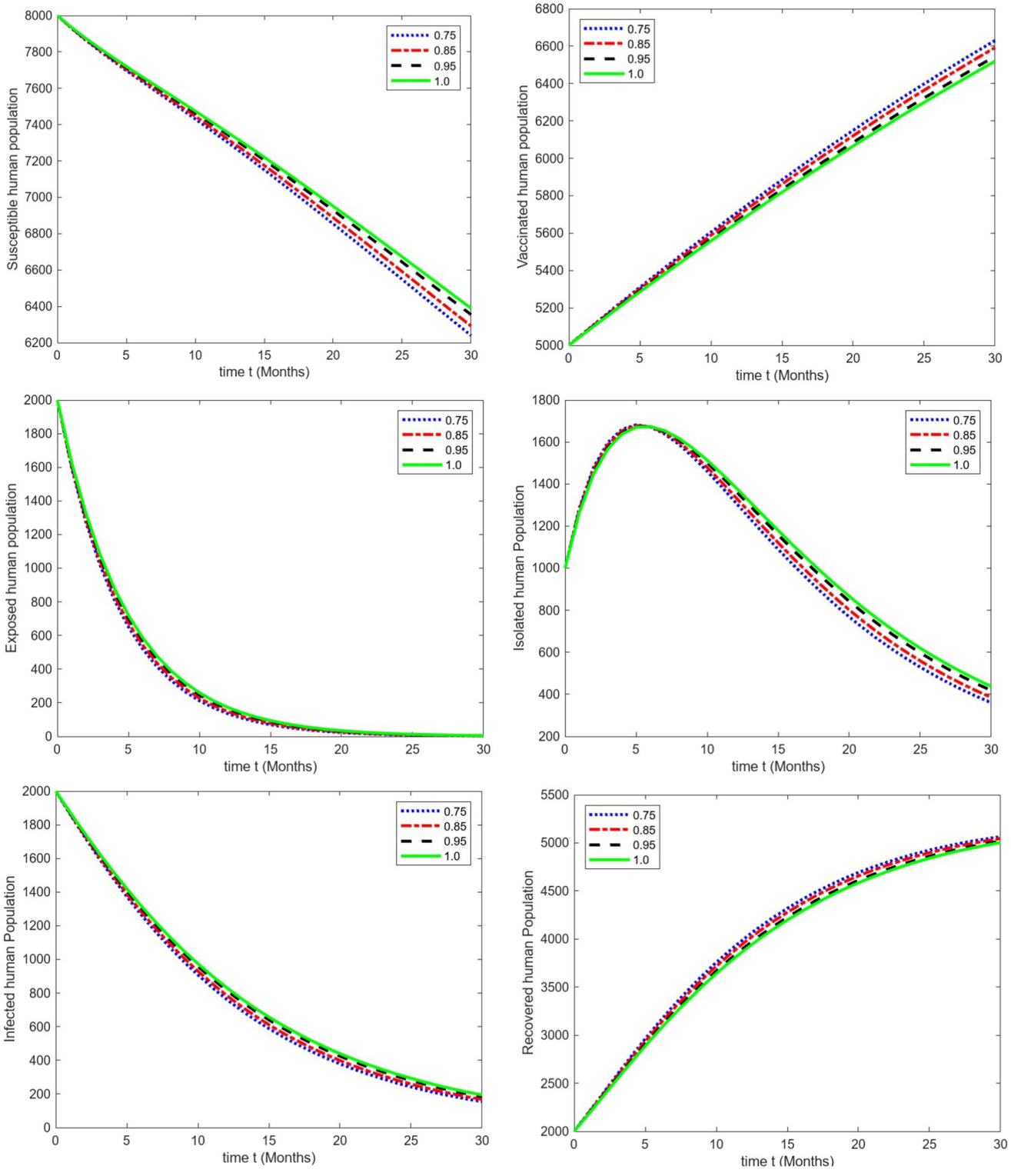

Fig. 2 Plotting numerical scheme given by Refs. 48–57 using different values of α.

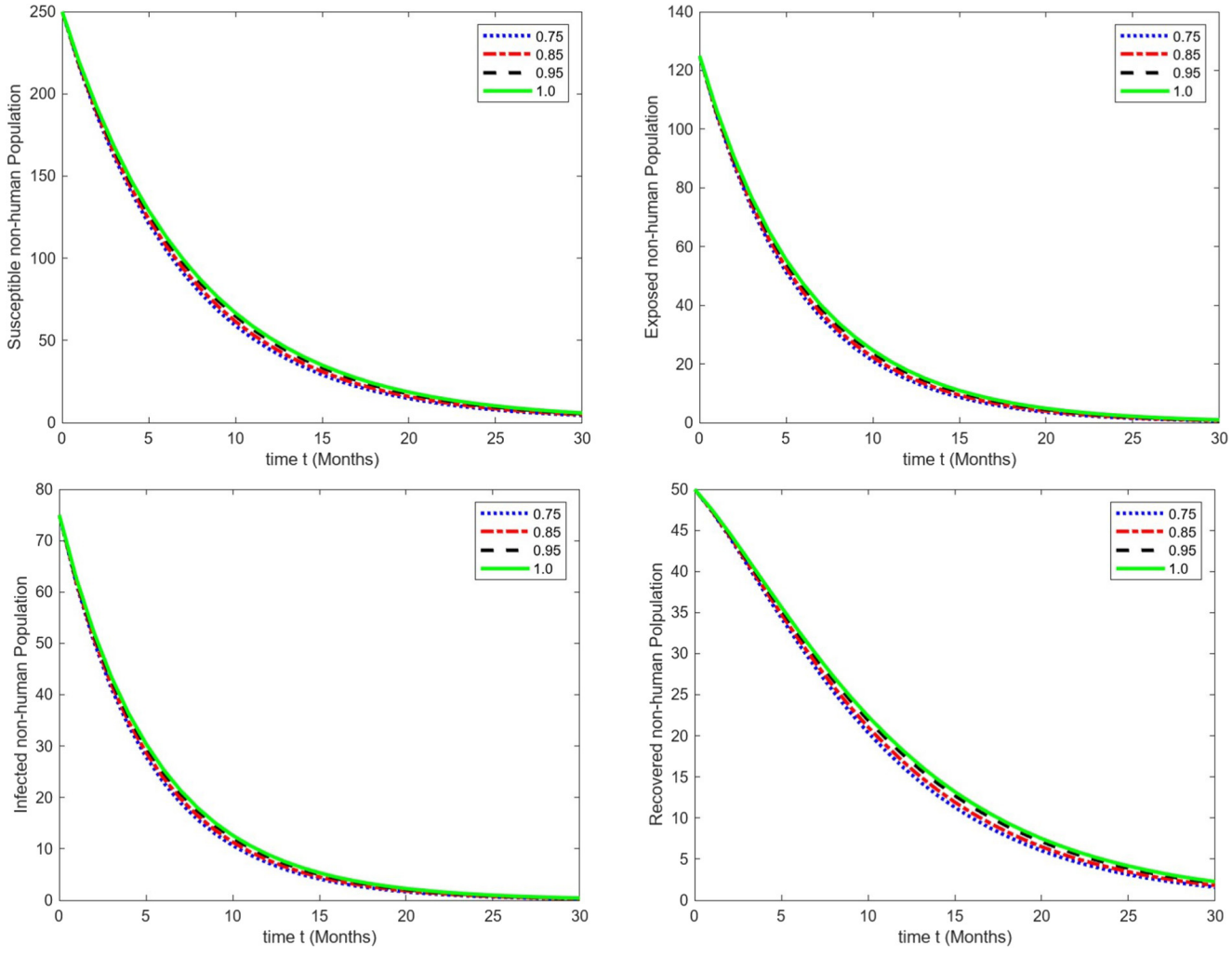

Fig. 2 *Continued*

$$\begin{cases} E_r(t_m) = E_r(0) + \chi^{1-\alpha}\dfrac{h^\alpha}{\Gamma(\alpha+2)}\big((m-1)^{\alpha+1} \\ \quad -(m-\alpha-1)m^\alpha\big)\Theta_8(t_0, E_r(t_0)) \\ \quad +\chi^{1-\alpha}\dfrac{h^\alpha}{\Gamma(\alpha+2)}\displaystyle\sum_{i=1}^{m-1}\big((m-i+1)^{\alpha+1} \\ \quad -2(m-1)^{\alpha+1}+(m-i-1)^{\alpha+1}\big)\Theta_8 \\ \quad \times(t_i, E_r(t_i)) + \chi^{1-\alpha}\dfrac{h^\alpha}{\Gamma(\alpha+2)}\Theta_8 \\ \quad \times\left(t_m, E_r(t_{m-1}) + \dfrac{h^\alpha}{\Gamma(\alpha+2)}\Theta_8 \right. \\ \quad \left. \times(t_{m-1}, E_r(t_{m-1}))\right), \end{cases} \tag{55}$$

$$\begin{cases} I_r(t_m) = I_r(0) + \chi^{1-\alpha}\dfrac{h^\alpha}{\Gamma(\alpha+2)}\big((m-1)^{\alpha+1} \\ \quad -(m-\alpha-1)m^\alpha\big)\Theta_9(t_0, I_r(t_0)) \\ \quad +\chi^{1-\alpha}\dfrac{h^\alpha}{\Gamma(\alpha+2)}\displaystyle\sum_{i=1}^{m-1}\big((m-i+1)^{\alpha+1} \\ \quad -2(m-1)^{\alpha+1}+(m-i-1)^{\alpha+1}\big)\Theta_9 \\ \quad \times(t_i, I_r(t_i)) + \chi^{1-\alpha}\dfrac{h^\alpha}{\Gamma(\alpha+2)}\Theta_9 \\ \quad \times\left(t_m, I_r(t_{m-1}) + \dfrac{h^\alpha}{\Gamma(\alpha+2)}\Theta_9 \right. \\ \quad \left. \times(t_{m-1}, I_r(t_{m-1}))\right), \end{cases} \tag{56}$$

$$\begin{cases} R_r(t_m) = R_r(0) + \chi^{1-\alpha}\dfrac{h^\alpha}{\Gamma(\alpha+2)}\big((m-1)^{\alpha+1} \\ \quad -(m-\alpha-1)m^\alpha\big)\Theta_{10}(t_0, R_r(t_0)) \\ \quad +\chi^{1-\alpha}\dfrac{h^\alpha}{\Gamma(\alpha+2)}\displaystyle\sum_{i=1}^{m-1}\big((m-i+1)^{\alpha+1} \\ \quad -2(m-1)^{\alpha+1}+(m-i-1)^{\alpha+1}\big)\Theta_{10} \\ \quad \times(t_i, R_r(t_i)) + \chi^{1-\alpha}\dfrac{h^\alpha}{\Gamma(\alpha+2)}\Theta_{10} \\ \quad \times\left(t_m, R_r(t_{m-1}) + \dfrac{h^\alpha}{\Gamma(\alpha+2)}\Theta_{10}\right. \\ \quad \left.\times(t_{m-1}, R_r(t_{m-1}))\right). \end{cases} \tag{57}$$

4.2. Results and Discussion

In this section, we take into account model (6) and generate the graphical output by applying the parameter values from Table 1. Prior articles on the monkeypox virus only covered the model using integer-order differential equations; however, this paper uses fractional-order derivatives which provide greater accuracy and predictability. The fractional-order derivative gives us the freedom to adjust the order to an arbitrary value, whichever fits the real data better. Furthermore, the model used in this paper can also be used for smallpox or chickenpox-like diseases.

In the case of fractional-order derivatives, we can change the α according to our requirements and can obtain a better approximation that is more in line with the real data. $\alpha = 1$ represents the first-order derivative, but since the real data does not always follow integer-order derivatives or the approximation done by integer-order derivatives is not that accurate. The graphs in Fig. 2 depict the same that we can adjust the outcome simply by altering the order of the derivative, allowing us to select an order that is consistent with the actual data, which is not possible with integer-order derivatives.

We run numerical simulations to evaluate the presented model on MATLAB version R2022b[33] using the corresponding preliminary values: $S_h(0) = 8000$, $V_h(0) = 5000$, $E_h(0) = 2000$, $Q_h(0) = 1000$, $I_h(0) = 2000$, $R_h(0) = 2000$, $S_r(0) = 250$, $E_r(0) = 125$, $I_r(0) = 75$, $R_r(0) = 50$. All initial values are obtained from Ref. 34. The approximations provided in Refs. 48–57 are shown as graphs with various fractional orders in Table 1.

In Fig. 2, We have provided the approximations for the various compartments' solutions to the given data and fractional orders.

5. CONCLUSION

To better explain the spread of monkeypox illness, a fractional compartmental model has been developed. Ten divisions make up the suggested paradigm, all of which are exclusive. Six sections have been created for the human species, with the vaccinated (V_h), exposed (E_h), and isolated human (Q_h) compartments joining the conventional susceptible population (S_h), infected humans (I_h), and recovered humans (R_h) compartments. In the same way, the non-human population is split into four categories: exposed (E_r), susceptible (S_r), infected (I_r), and recovered (R_r).

We have also established the suggested model's fundamental features. The basic replication number was calculated using the next-generation matrix method. The suggested model has two equilibrium points: an endemic equilibrium point and a disease-free equilibrium point.

The stability requirements for both equilibria have been determined. With the assistance of fixed point theory, we have also analyzed the solution's existence and uniqueness. The numerical technique that was utilized to plot the graphs was generated using fractional Euler's method and a modified trapezoidal rule.

The predictability of the model can be further improved by using delay differential and modified Caputo fractional derivative in addition to the fractional-order derivative that has been utilized here.

As a result of the simulation, it is clear that isolation of infected persons, as well as vaccination, plays an important role in managing and controlling the monkeypox virus.

ACKNOWLEDGMENTS

Jaskirat Pal Singh, the author, gratefully acknowledges the CSIR Research Grant: 09/1051(12023)/ 2021- EMR-I. The author Sachin Kumar acknowledges the financial support given under the Scheme "Fund for Improvement of S&T Infrastructure (FIST)" of the Department of Science & Technology (DST), Government of India, as demonstrated by letter number SR/FST/MS-I/2021/104. This study is supported via funding from Prince

Sattam bin Abdulaziz University project number (PSAU/2023/R/1444).

ORCID

J. P. Singh https://orcid.org/0000-0002-8938-1289
S. Kumar https://orcid.org/0000-0001-6883-7788
D. Baleanu https://orcid.org/0000-0002-0286-7244
K. S. Nisar https://orcid.org/0000-0001-5769-4320

REFERENCES

1. CDC *et al.*, Update: Multistate outbreak of monkeypox–Illinois, Indiana, Kansas, Missouri, Ohio, and Wisconsin, 2003, *Morb. Mortal Wkly. Rep.* **52**(24) (2003) 561–564.
2. Z. Jezek, M. Szczeniowski, K. Paluku, M. Mutombo and B. Grab, Human monkeypox: Confusion with chickenpox, *Acta Tropica* **45**(4) (1988) 297–307.
3. P. V. Magnus, E. K. Andersen, K. B. Petersen and A. Birch-Andersen, A pox-like disease in cynomolgus monkeys, *Acta Pathol. Microbiol. Scand.* **46**(2) (1959) 156–176.
4. I. Ladnyj, P. Ziegler and E. Kima, A human infection caused by monkeypox virus in Basankusu Territory, Democratic Republic of the Congo, *Bull. World Health Organ.* **46**(5) (1972) 593.
5. H. Adler, S. Gould, P. Hine, L. B. Snell, W. Wong, C. F. Houlihan, J. C. Osborne, T. Rampling, M. B. Beadsworth, C. J. Duncan *et al.*, Clinical features and management of human monkeypox: A retrospective observational study in the UK, *Lancet Infect Dis.* **22**(7) (2022) e177.
6. G. D. Huhn, A. M. Bauer, K. Yorita, M. B. Graham, J. Sejvar, A. Likos, I. K. Damon, M. G. Reynolds and M. J. Kuehnert, Clinical characteristics of human monkeypox, and risk factors for severe disease, *Clin. Infect. Dis.* **41**(12) (2005) 1742–1751.
7. B. E. Cunha, Monkeypox in the United States: an occupational health look at the first cases, *AAOHN J.* **52**(4) (2004) 164–168.
8. K. D. Reed, J. W. Melski, M. B. Graham, R. L. Regnery, M. J. Sotir, M. V. Wegner, J. J. Kazmierczak, E. J. Stratman, Y. Li, J. A. Fairley *et al.*, The detection of monkeypox in humans in the western hemisphere, *N. Engl. J. Med.* **350**(4) (2004) 342–350.
9. M. G. Reynolds, K. L. Yorita, M. J. Kuehnert, W. B. Davidson, G. D. Huhn, R. C. Holman and I. K. Damon, Clinical manifestations of human monkeypox influenced by route of infection, *J. Infect. Dis.* **194**(6) (2006) 773–780.
10. D. W. Grosenbach, K. Honeychurch, E. A. Rose, J. Chinsangaram, A. Frimm, B. Maiti, C. Lovejoy, I. Meara, P. Long and D. E. Hruby, Oral tecovirimat for the treatment of smallpox, *N. Engl. J. Med.* **379**(1) (2018) 44–53.
11. G. Chittick, M. Morrison, T. Brundage and W. G. Nichols, Short-term clinical safety profile of brincidofovir: A favorable benefit–risk proposition in the treatment of smallpox, *Antiviral Res.* **143** (2017) 269–277.
12. D. Delaune and F. Iseni, Drug development against smallpox: Present and future, *Antimicrob. Agents Chemother.* **64**(4) (2020) e01683–19.
13. J. Djordjevic, C. J. Silva and D. F. Torres, A stochastic SICA epidemic model for HIV transmission, *Appl. Math. Lett.* **84** (2018) 168–175.
14. F. Ndaïrou, I. Area, J. J. Nieto, C. J. Silva and D. F. Torres, Mathematical modeling of Zika disease in pregnant women and newborns with microcephaly in Brazil, *Math. Methods Appl. Sci.* **41**(18) (2018) 8929–8941.
15. A. Rachah and D. F. Torres, Dynamics and optimal control of Ebola transmission, *Math. Comput. Sci.* **10**(3) (2016) 331–342.
16. R. Magin, Fractional calculus in bioengineering, part 1, *Crit. Rev. Biomed. Eng.* **32**(1) (2004) 1–104.
17. D. Baleanu, H. Mohammadi and S. Rezapour, A mathematical theoretical study of a particular system of Caputo–Fabrizio fractional differential equations for the Rubella disease model, *Adv. Differ. Eq.* **2020**(1) (2020) 1–19.
18. R. Hilfer, *Applications of Fractional Calculus in Physics* (World Scientific, 2000).
19. I. Podlubny, *Fractional Differential Equations*: *An Introduction to Fractional Derivatives*, *Fractional Differential Equations*, *to Methods of their Solution and Some of their Applications* (Elsevier, 1998).
20. D. Baleanu, A. Jajarmi, S. S. Sajjadi and J. H. Asad, The fractional features of a harmonic oscillator with position-dependent mass, *Commun. Theor. Phys.* **72**(5) (2020) 055002.
21. D. Baleanu, A. Jajarmi, H. Mohammadi and S. Rezapour, A new study on the mathematical modelling of human liver with Caputo–Fabrizio fractional derivative, *Chaos*, *Solitons Fractals* **134** (2020) 109705.
22. A. Jajarmi, A. Yusuf, D. Baleanu and M. Inc, A new fractional HRSV model and its optimal control: A non-singular operator approach, *Physica A* **547** (2020) 123860.
23. J. Gómez-Aguilar, J. Rosales-García, J. Bernal-Alvarado, T. Córdova-Fraga and R. Guzmán-Cabrera, Fractional mechanical oscillators, *Rev. Mex. Fis.* **58**(4) (2012) 348–352.
24. D. Baleanu, F. A. Ghassabzade, J. J. Nieto and A. Jajarmi, On a new and generalized fractional model for a real cholera outbreak, *Alex. Eng. J.* **61**(11) (2022) 9175–9186.

25. S. G. Samko, A. A. Kilbas, O. I. Marichev *et al.*, *Fractional Integrals and Derivatives* (Gordon and Breach Science Publishers, Yverdon Yverdon-Les-Bains, Switzerland, 1993).
26. O. Diekmann, J. Heesterbeek and M. G. Roberts, The construction of next-generation matrices for compartmental epidemic models, *J. R. Soc. Interface* **7**(47) (2010) 873–885.
27. O. J. Peter, R. Viriyapong, F. A. Oguntolu, P. Yosyingyong, H. O. Edogbanya and M. O. Ajisope, Stability and optimal control analysis of a SCIR epidemic model, *J. Math. Comput. Sci.* **10**(6) (2020) 2722–2753.
28. P. Van den Driessche and J. Watmough, Further notes on the basic reproduction number, in *Mathematical Epidemiology* (Springer, 2008), pp. 159–178.
29. O. J. Peter, S. Kumar, N. Kumari, F. A. Oguntolu, K. Oshinubi and R. Musa, Transmission dynamics of Monkeypox virus: A mathematical modelling approach, *Model. Earth Syst. Environ.* **8** (2022) 3423–3434.
30. P. Samui, J. Mondal and S. Khajanchi, A mathematical model for COVID-19 transmission dynamics with a case study of India, *Chaos, Solitons & Fractals* **140** (2020) 110173.
31. C. Castillo-Chavez, Z. Feng, W. Huang *et al.*, On the computation of R_o and its role on global stability, in *Mathematical Approaches for Emerging and Reemerging Infectious Diseases*: *An Introduction*, **1** (Springer, 2002), pp. 229–250.
32. A. Hurwitz *et al.*, On the conditions under which an equation has only roots with negative real parts, *Sel. Papers Math. Trends Control Theory* **65** (1964) 273–284.
33. The Mathworks, Inc., Natick, Massachusetts, MATLAB version 9.13.0.2049777 (R2022b) (2022).
34. S. Usman, I. I. Adamu *et al.*, Modeling the transmission dynamics of the monkeypox virus infection with treatment and vaccination interventions, *J. Appl. Math. Phys.* **5**(12) (2017) 2335.
35. C. Bhunu and S. Mushayabasa, Modelling the transmission dynamics of pox-like infections, *IAENG Int. J. Appl. Math.* **41**(2) (2011).